

Multiscale Image Analysis of Calcium Dynamics in Cardiac Myocytes

Alexander Vallmitjana^{1,S,*}, Raúl Benítez²

1. Biomedical Engineering Department, University of California, Irvine 92697, USA

2. Automatic Control Department, Universitat Politècnica de Catalunya, Barcelona 08034, Spain

(*) E-mail: avallmit@uci.edu

S: SEDOPTICA member

Received: 09/11/2021 Accepted: 24/06/2022

DOI: 10.7149/OPA.55.2.51076

ABSTRACT:

Cardiac myocytes are the muscle cells that build up heart tissue and provide the mechanical action to pump blood by synchronously contracting at every heartbeat. Heart muscle contraction is regulated by intracellular calcium concentration which exhibits a complex spatio-temporal dynamical behavior at the molecular, cellular and tissue levels. Details of such dynamical patterns are closely related to the mechanisms responsible for cardiovascular diseases, the single largest cause of death in the developed countries. The emerging field of translational cardiology focuses on the study of how such mechanisms connect and influence each other across spatial and temporal scales, eventually yielding to a certain clinical condition. To study such calcium dynamics in cardiac myocytes, we benefit from the recent advances in the field of experimental cell physiology. Fluorescence microscopy allows us to observe the distribution of calcium in the cell with a spatial resolution below one micron and a frame rate around one millisecond, thus providing a very accurate monitoring of calcium fluxes in the cell. The aim of the thesis summarized in this paper, was to develop image processing computational techniques for extracting quantitative data of physiological relevance from fluorescence confocal microscopy images at different scales. The two main subjects covered in the thesis were image segmentation and classification methods applied to fluorescence microscopy imaging of cardiac myocytes and calcium imaging. These methods were applied to a variety of problems involving different space and time scales, such as the localization of molecular receptors, the detection and characterization of spontaneous calcium-release events, and the propagation of calcium waves across a culture of cardiac cells. The following is a summary of the thesis as a consequence of having been awarded the 7th Justiniano Casas Award accessit by the Sociedad Española de Óptica.

Key words: Calcium Imaging, Fluorescence Microscopy, Image Processing

REFERENCES

- [1] D. M. Bers, "Cardiac Excitation Contraction Coupling," *Nature* 415, 198–205 (2002).
- [2] A. Fabiato, "Calcium-Induced Release of Calcium from the Cardiac Sarcoplasmic-Reticulum," *Am. J. Physiol.* 245, C1–C14 (1983).
- [3] D. M. Jameson, *Introduction to Fluorescence* (Taylor & Francis, 2014).
- [4] A. Vallmitjana, "Multiscale Image Analysis of Calcium Dynamics in Cardiac Myocytes," PhD Thesis, Dep. d'Enginyeria Sist. Automàtica i Informàtica Ind. Univ. Politec. Catalunya (2017).
- [5] M. A. Walker, T. Kohl, S. E. Lehnart, J. L. Greenstein, W. J. Lederer, and R. L. Winslow, "On the Adjacency Matrix of RyR2 Cluster Structures," *Plos Comput. Biol.* 11, 1–21 (2015).
- [6] T. M. Hoang-Trong, A. Ullah, and M. S. Jafri, "Calcium Sparks in the Heart: Dynamics and Regulation," *Res. Rep. Biol.* 6, 203–214 (2015).
- [7] F. Hiess, A. Vallmitjana, R. Wang, H. Cheng, H. E. D. J. ter Keurs, J. Chen, L. Hove-Madsen, R. Benitez, S. R. W. Chen, and R. Benítez, "Distribution and function of cardiac ryanodine receptor clusters in live ventricular myocytes," *J. Biol. Chem.* 290, 20477–20487 (2015).
- [8] C. Nolla-Colomer, "Anàlisi de patrons funcionals i estructurals en la regulació del calci en les cèl·lules cardíques," PhD Thesis, Dep. d'Enginyeria Sist. Automàtica i Informàtica Ind. Univ. Politec. Catalunya (2021).



- [9] X. Zhong, B. Sun, A. Vallmitjana, T. Mi, W. Guo, M. Ni, R. Wang, A. Guo, H. J. Duff, A. M. Gillis, L.-S. Song, L. Hove-Madsen, R. Benitez, and S. R. W. W. Chen, "Suppression of Ryanodine Receptor Function Prolongs Ca²⁺ Release Refractoriness and Promotes Cardiac Alternans in Intact Hearts," *Biochem. J.* 473, 3951–3964 (2016).
- [10] F. Hiess, P. Detampel, C. Nolla-Colomer, A. Vallmitjana, A. Ganguly, M. Amrein, H. E. D. J. ter Keurs, R. Benítez, L. Hove-Madsen, and S. R. W. W. Chen, "Dynamic and Irregular Distribution of RyR2 Clusters in the Periphery of Live Ventricular Myocytes," *Biophys. J.* 114, 343–354 (2018).
- [11] E. Chudin, J. Goldhaber, A. Garfinkel, J. Weiss, and B. Kogan, "Intracellular Ca²⁺ dynamics and the stability of ventricular tachycardia," *Biophys. J.* 77, 2930–2941 (1999).
- [12] H. Ishida, C. Genka, Y. Hirota, H. Nakazawa, and W. H. Barry, "Formation of Planar and Spiral Ca²⁺ Waves in Isolated Cardiac Myocytes," *Biophys. J.* 77, 2114–2122 (1999).
- [13] Y. Bai, P. P. Jones, J. Guo, X. Zhong, R. B. Clark, Q. Zhou, R. Wang, A. Vallmitjana, R. Benitez, L. Hove-madsen, L. Semeniuk, A. Guo, L. Song, H. J. Duff, and S. R. W. Chen, "Phospholamban knockout breaks arrhythmogenic Ca²⁺ waves and suppresses catecholaminergic polymorphic ventricular tachycardia in mice," *Circ. Res.* 113, 517–526 (2013).
- [14] A. Herraiz-Martínez, J. Álvarez-García, A. Llach, C. E. Molina, J. Fernandes, A. Ferrero-Gregori, C. Rodríguez, A. Vallmitjana, R. Benítez, J. Padró, J. Martínez-González, J. Cinca, and L. Hove-Madsen, "Ageing is associated with deterioration of calcium homeostasis in isolated human right atrial myocytes," *Cardiovasc. Res.* 106, 76–86 (2015).
- [15] A. Herraiz-Martínez, A. Llach, C. Tarifa, J. Gandía, V. Jiménez-Sabado, E. Lozano-Velasco, S. A. S. A. Serra, A. Vallmitjana, E. Vázquez Ruiz De Castroviejo, R. Benítez, A. Aranega, C. Muñoz-Guijosa, D. Franco, J. Cinca, and L. Hove-Madsen, "The 4q25 variant rs13143308T links risk of atrial fibrillation to defective calcium homoeostasis," *Cardiovasc. Res.* 115, 578–589 (2019).
- [16] C. Nolla-Colomer, S. Casabella-Ramon, V. Jimenez-Sabado, A. Vallmitjana, C. Tarifa, A. Herraiz-Martínez, A. Llach, M. Tauron, J. Montiel, J. Cinca, S. R. W. Chen, R. Benitez, and L. Hove-Madsen, "B2-adrenergic Stimulation Potentiates Spontaneous Calcium Release by Increasing Signal Mass and Co-activation of Ryanodine Receptor Clusters," *Acta Physiol.* 234, e13736 (2021).
- [17] X. Zhong, A. Vallmitjana, B. Sun, Z. Xiao, W. Guo, J. Wei, M. Ni, Y. Chen, E. R. O'Brien, A. M. Gillis, M. Hoshijima, H. Takeshima, L. Hove-Madsen, R. Benitez, D. Belke, and S. R. W. Chen, "Reduced expression of cardiac ryanodine receptor protects against stress-induced ventricular tachyarrhythmia, but increases the susceptibility to cardiac alternans," *Biochem. J.* 475, 169–183 (2018).
- [18] A. Vallmitjana, A. Civera-Tregon, J. Hoenicka, F. Palau, and R. Benitez, "Motion estimation of subcellular structures from fluorescence microscopy images," *Proc. Annu. Int. Conf. IEEE Eng. Med. Biol. Soc.* EMBS 4419–4422 (2017).
- [19] A. Civera-Tregón, L. Domínguez, P. Martínez-Valero, C. Serrano, A. Vallmitjana, R. Benítez, J. Hoenicka, J. Satrústegui, and F. Palau, "Mitochondria and calcium defects correlate with axonal dysfunction in GDAP1-related Charcot-Marie-Tooth mouse model," *Neurobiol. Dis.* 152, 105300 (2021).
- [20] L. Breiman, "Random forests," *Mach. Learn.* 45, 5–32 (2001).
- [21] M. Barriga, R. Cal, N. Cabello, A. Llach, A. Vallmitjana, R. Benitez, L. Badimon, J. Cinca, V. Llorente-Cortes, L. Hove-Madsen, and R. Benítez, "Low density lipoproteins promote unstable calcium handling linked to reduced SERCA2 and connexin 40 expression in cardiomyocytes," *PLoS One* 8, e58128–e58128 (2013).
- [22] C. E. Molina, A. Llach, A. Herraiz-Martínez, C. Tarifa, M. Barriga, R. F. Wiegerinck, J. Fernandes, N. Cabello, A. Vallmitjana, R. Benitez, J. Montiel, J. Cinca, and L. Hove-Madsen, "Prevention of adenosine A2A receptor activation diminishes beat-to-beat alternation in human atrial myocytes," *Basic Res. Cardiol.* 111, 5 (2016).
- [23] J. Rivera-Torres, C. J. C. J. Calvo, A. Llach, G. Guzmán-Martínez, R. Caballero, C. González-Gómez, L. J. L. J. Jiménez-Borreguero, J. A. Guadix, F. G. F. G. Osorio, C. López-Otín, A. Herraiz-Martínez, N. Cabello, A. Vallmitjana, R. Benítez, L. B. L. B. Gordon, J. Jalife, J. M. J. M. Pérez-Pomares, J. Tamargo, E. Delpón, L. Hove-Madsen, D. Filgueiras-Rama, and V. Andrés, "Cardiac electrical defects in progeroid mice and Hutchinson-Gilford progeria syndrome patients with nuclear lamina alterations," *Proc. Natl. Acad. Sci.* 113, E7250–E7259 (2016).
- [24] M. A. Colman, "The Multiple Mechanisms of Spatially Discordant Alternans in the Heart," *Biophys. J.* 118, 2336–2338 (2020).
- [25] A. Vallmitjana, M. Barriga, Z. Nenadic, A. Llach, E. Alvarez-Lacalle, L. Hove-Madsen, and R. Benitez, "Identification of intracellular calcium dynamics in stimulated cardiomyocytes," *Annu Int Conf IEEE Eng Med Biol Soc.* 2010, 68–71 (2010).
- [26] B. Sun, J. Yao, M. Ni, J. Wei, X. Zhong, W. Guo, L. Zhang, R. Wang, D. Belke, Y.-X. Chen, K. V. V. Lieve, A. K. Broendberg, T. M. Roston, I. Blankoff, J. A. Kammeraad, J. C. von Alvensleben, J. Lazarte, A. Vallmitjana, L. J. Bohne, R. A. Rose, R. Benitez, L. Hove-Madsen, C. Napolitano, R. A. Hegele, M. Fill, S. Sanatani, A. A. M. Wilde, J. D. Roberts, S. G. Priori, H. K. Jensen, and S. R. W. Chen, "Cardiac ryanodine receptor calcium release deficiency syndrome," *Sci. Transl. Med.* 13, eaba7287 (2021).
- [27] B. Sun, J. Wei, X. Zhong, W. Guo, J. Yao, R. Wang, A. Vallmitjana, R. Benitez, L. Hove-Madsen, and S. R. W. Chen, "The cardiac ryanodine receptor, but not sarcoplasmic reticulum Ca²⁺-ATPase, is a major determinant of Ca²⁺ alternans in intact mouse hearts," *J. Biol. Chem.* 293, jbc.RA118.003760 (2018).
- [28] J. Wei, J. Yao, D. Belke, W. Guo, X. Zhong, B. Sun, R. Wang, J. P. Estillore, A. Vallmitjana, R. Benitez, L. Hove-Madsen, E. Alvarez-Lacalle, B. Echebarria, and S. W. Chen, "Ca²⁺ -CaM Dependent Inactivation of RyR2 Underlies Ca²⁺ Alternans in Intact Heart," *Circ. Res.* 128, 63–83 (2021).
- [29] A. Vallmitjana, M. Barriga, L. Hove-Madsen, and R. Benitez, "Multilevel analysis of calcium dynamics in stimulated cultures of cardiomyocytes," *Annu Int Conf IEEE Eng Med Biol Soc.* 2013, 6514–6517 (2013).
- [30] L. Hove-Madsen, A. Vallmitjana, and R. Benitez, "Método implementado por ordenador para caracterización dinámica de células en cultivos celulares y programas informáticos para llevar a cabo el método," patent ES2532746B1 (2016).



1. Introduction

The onset of the information age has made image processing and analysis to become a key player in the field of biology. As a result of the combined progress of microscopy and computer engineering, current researchers are producing huge amounts of data, significantly more than they can store and analyze, especially considering the manual and time-consuming traditional analysis techniques. Techniques such as segmenting (Fig. 1), labelling or counting objects in an image and measuring their morphological features have historically been human dependent and subjective, whereas now, with the aid of software tools, they are becoming objective and more reproducible. Results that were previously limited to qualitative observation are now gradually becoming quantitative, demonstrating the need for bridge disciplines: disciplines like biomedical engineering, that are halfway between the classical science pillars, cover the gap in this case between researchers applying bio-imaging and the advanced mathematical and computational tools available.



Fig. 1. Segmentation is a subjective task. A) Photograph of a chapel (Tarrés, Lleida). B) Ask a computer to identify 3 regions (k-means into 3 clusters). C) Ask a human to identify 3 regions.

1.a. Calcium and Cardiac Myocytes

Cardiac myocytes are elongated cells attached to one another in the longitudinal direction forming the cardiac muscular fibers (Fig. 2). Each of them is around $100\text{ }\mu\text{m}$ long and $25\text{ }\mu\text{m}$ wide with the human heart consisting of 10^9 cardiac myocytes all contracting at each heartbeat, pumping around 7000 liters of blood a day, and producing a total of around 3×10^9 beats in an average human lifetime. Contraction of myocytes is dictated via electrical stimulus, with the process converting this electrical stimulus into mechanical force called excitation-contraction coupling [1]. The charge carriers at the cellular level are ions of different chemical elements, most notably Na^+ , K^+ , Ca^{2+} , Cl^- , are responsible for carrying electric charge by flowing through specific protein complexes embedded in the cellular membrane, complexes in turn regulated by local conditions. In the case of cardiac myocytes, the ion that is mainly responsible for regulation of contraction is the calcium ion.

Myocytes contain a structure of interleaved protein filaments (actin and myosin, among others) that acts as the cell skeleton or scaffolding. This structure can slide in between itself acting as the contractile machinery that allows the cell to shorten its length. This motion is triggered by the presence of Ca^{2+} . During contraction, myocytes undergo a process called calcium-induced calcium release [2]. Specifically, myocytes have a Ca^{2+} reservoir inside that contributes to raising the concentration of Ca^{2+} by a factor of 10^4 above the concentration they would reach by just letting Ca^{2+} flow from the outside. This reservoir is the sarcoplasmic reticulum which releases large amounts of Ca^{2+} into the cytoplasm. This release is triggered by a small increase in Ca^{2+} concentration originated from an outside influx of Ca^{2+} . The two main transmembrane proteins that allow this calcium flux from the sarcoplasmic reticulum are the ryanodine receptor (RyR2) for the release flux and the SERCA pump for the subsequent regathering back into the reticulum.

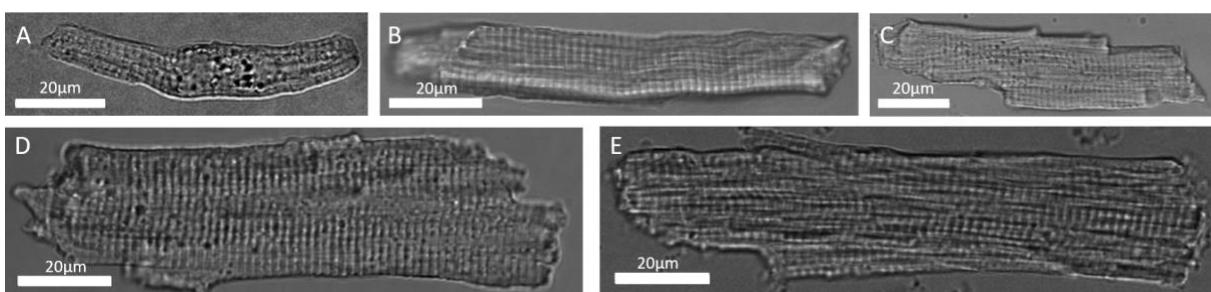


Fig. 2. Cardiac myocytes under a transmission microscope. Human (A) and pig (B) atrial. Rat (C), rabbit (D) and mouse (E) ventricular.

The cycle each cardiac myocyte undergoes with each heartbeat can be summarized as: 1) In the resting state, the myocyte keeps an electrical membrane potential of around -90 mV. The cell is polarized, with an excess of negative charge. 2) A variation in the extracellular charge (originating at neighboring cells) triggers a depolarization of the cell, allowing positive ions through the membrane, mainly Na^+ and K^+ . 3) Membrane potential depolarizes and reaches a value of up to +50 mV. At this point Ca^{2+} starts to enter the cell while K^+ are ejected, fixing the positive voltage value, and starting the calcium-induced calcium release process. This initiates contraction of the myocyte. 4) Finally, Ca^{2+} is collected back into the sarcoplasmic reticulum and ejected out of the cell, which returns to the negative potential resting state.

1.b. Calcium Imaging

Fluorescence is a natural phenomenon by which a molecule will absorb light of a certain energy and re-emit it in a lower energy after some internal atomic non-radiative transitions. The term was coined by Stokes in 1852 although its first recorded description is from the 1560s by a Spanish missionary on the wood the Aztecs named *coatl* [3]. In fluorescence microscopy, a specimen is loaded with fluorophore, which binds to the structure of interest and then illuminates the sample with light of the appropriate wavelength for the absorption by the fluorophore. Its emission is then recorded using a filter to block light of all other wavelengths. For the case of measuring Ca^{2+} concentration there are many available fluorophores with one common example being Fluo-4. The excitation wavelength peak of Fluo-4 is 494 nm and the emission peak is 516 nm. To use this fluorophore, we would illuminate the sample with laser of a wavelength around 494 nm, record the emission through a microscope with a filter around 516 nm. The intensity of light recorded would then be directly proportional to the intracellular Ca^{2+} concentration.

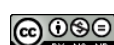
The magnification power of a microscope is defined as the ratio between the angle under which we see an object through the microscope and the angle under which we would see the object without the microscope (at the closest possible distance the eye can focus it, standardized to 25 mm). This magnification can be achieved using a single convergent lens but to a much greater degree by combining a set of lenses. A scanning microscope relies on two mirrors each mounted on a motor that are used to sequentially excite the sample. Because the excitation source rasterizes the sample in the plane perpendicular to the optical path (x-y plane) in a point-by-point fashion, this allows the use of ultrasensitive devices like photomultiplier tubes or avalanche photo-diodes. The scanning setup also allows for the presence of a confocal pinhole, a tiny aperture situated in the optical path of the emitted light that crops out emission from out-of-focus regions of the sample, achieving high optical slicing in the z-direction. In this manner, each image is obtained by scanning an x-y plane of the sample and by moving the sample up or down and scanning another image off a parallel plane to the first one. Obtaining a series of stacks through this approach allows for reconstruction of the sample in three dimensions.

Due to the wave nature of light, there are some considerations to be made when imaging objects the size of which is close to the wavelength of the light we are using to view them. Diffraction and interference are the main effects that result in an infinitely small point-source of light appearing as a diffraction pattern with a certain physical extension (the system's point spread function, PSF). Therefore, the images are composed by the sample being convolved by the diffraction pattern, the PSF. These patterns, in turn, depend on the size and shape of the device's aperture, the wavelength of the light and the medium the light is travelling through. The diffraction limit of an optical system is approximated by Abbe's formula and defines the smallest size resolvable by the optical system. Typically, in fluorescence microscopy, the diffraction limit is around the quarter of a micron, 250 nm.

1.c. Problem Diversity

Scanning techniques can be very limiting when recording the evolution of a sample, since the time needed to record the whole scene limits the frame rate of the final sequence. This is the reason why line scans were first introduced. The technique consists in scanning a single line in the sample at each frame. The result is, instead of a series of 2D images forming a film, a set of 1D lines that can be arranged to form a 2D image with one dimension being space and the other being time. This technique allows for a greater temporal resolution at the cost of losing a spatial dimension.

Including the line scan, there are a variety of imaging methods available. For dynamic temporal sequences one can do image sequences (x-y-t) *i.e.* a traditional movie, or line scans (x-t). For static imaging, one can



attain single slice images (x-y), or stacks of images at different heights (x-y-z). Hence we are dealing with a great diversity only in image formats. Adding the habitual data variability, instrumental, experimental or biological noise, and the many different experimental conditions, (physical lab conditions, sampling rate and spatial resolution, image formats and types), we are dealing with a large inter- and intra- experiment variability.

In addition, we are dealing with great variety of dynamics and patterns. A 10^3 -fold temporal range in calcium events, from the millisecond of the calcium unit release to the second where the heart beat takes place. A 10^6 -fold spatial range, from the nanometer of the molecular scale to the millimeter of the tissue scale (hence the thesis title with the term multiscale). A scale integration is required that connects molecular, sub-cellular, cellular and multicellular cultures. This thesis [4] is an attempt to connect the molecular scale to the tissue scale by developing a set of tools for signal and image processing that can account for the great variability in the data and can, automatically and above all rapidly, deal with the huge amounts of data that is produced.

2. Results

2.a. Molecular Scale

The Ryanodyne Receptor (RyR2) is a transmembrane protein acting as a calcium channel in the sarcoplasmic reticulum's (SR) membrane. Its role in the calcium-induced calcium release process is to mediate the massive release of calcium ions into the cytosol. Its name is due to ryanodine, an alkaloid found in a Caribbean plant *ryania speciosa*, which has nothing to do with cardiac function other than its toxicity to mammals for it blocks the RyR, and thus the historical name for the protein. RyR2 is the isoform of the protein found in cardiac cells. They are grouped in clusters, each containing a number ranging from a few dozen [5] to a few hundred [6], with the clusters distributed over the SR which at the same time is evenly distributed throughout the myocyte. It is well known that calcium release through the RyR2 plays a crucial role in the regulation of intracellular calcium and cardiac contraction and that some heart diseases are linked to mutations in the RyR2. However, little is known about the 3D distribution of RyR2 clusters throughout the cell and if they are the only agents responsible for calcium release from the sarcoplasmic reticulum. Therefore, the RyR2 is currently a common focus of study in many research groups, and the development of computational techniques for the detection of RyR2 clusters from fluorescence imaging is currently highly relevant. Our collaborators genetically engineered a mouse family line to express green fluorescent protein at the RyR2. As RyR2 are objects some ten times smaller than the diffraction limit of optical microscopes, they appear as blobs a little larger than the size of the system's PSF (see Fig. 3, BCDE).

We developed a simple and effective way to localize these structures in an image by performing a search for local brightness intensity maxima. To deal with noise, we used a Gaussian filter of the same size as the PSF of the system. The reason is two-fold; the 2D Gaussian is a good approximation of the PSF and it adjusts nicely to the image wherever clusters are located and, in this manner, RyR clusters will be enhanced while at the same time the whole image will be smoothed out reducing the number of false detections when localizing the clusters. Our cluster detection method combined a search for zero gradient with watershed-based method and was used extensively in multiple applications, ranging from analyzing its distribution and function [7] to relating RyR2 activation to calcium release events [8,9].

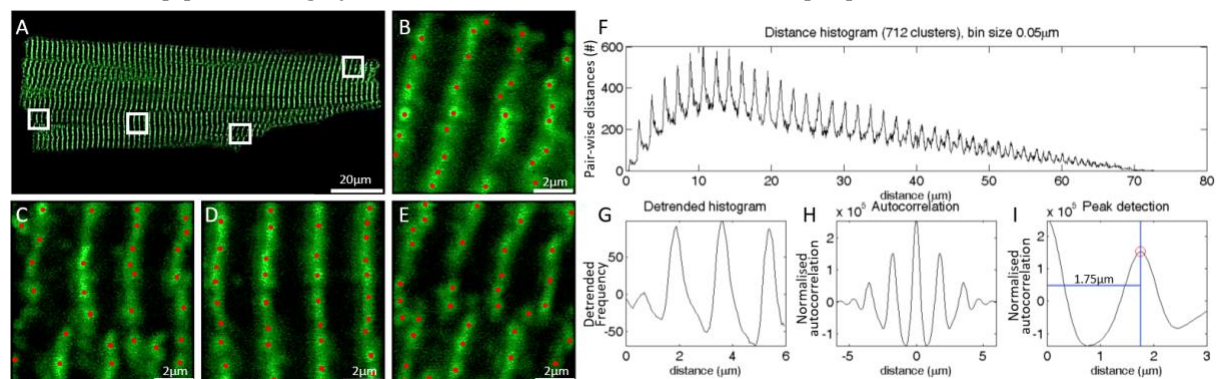


Fig. 3 A) RyR2-labeled mouse ventricular myocyte. B-E) Selected regions with the detected RyR2 locations. F) Histogram of pairwise distances between clusters. Detrended (G) and autocorrelated histogram (H) from which average z-line distance is obtained (I).

Z-lines are the name given to the observed dark lines between sarcomeres when viewing a myocyte under the microscope. They correspond to the place where actin molecules are bound together in the contractile machinery of a myocyte, and define a visual perception rather than a structural component of a myocyte. The distance between Z-lines in a myocyte provides information about the grade of contraction of a myocyte and so the measurement of this distance is relevant when studying myocytes. The reticular distribution of RyR2 clusters corresponds to the periodic distribution of actin myosin filaments and, for this reason, the distance between bands of RyR2 clusters corresponds to the Z-line distance (see Fig. 3A). Our proposed method for automated measurement of Z-line distance was a statistical approach which makes use of the fast algorithms available for computing pairwise distances between a set of objects, in this case between RyR2 clusters. If an image has N detected clusters, the number of pair-wise distances is $(N^2-N)/2$. Taking the histogram of the measured distances (Fig. 3F), due to the periodic distribution of clusters, this histogram produces a series of maxima matching the multiples of the Z-line distance. By autocorrelating this histogram (cross-correlation by itself, Fig. 3H), the position of the first peak provides the averaged most present distance in the image and therefore a mean Z-line distance by taking into account all clusters (Fig. 3I). This method was used in order to characterize RyR2 distribution and colocalize it to calcium release events [7,10].

2.b. Sub-Cellular Scale

During cardiac contraction each myocyte undergoes *calcium-induced calcium release*, described previously. It is a complex process in which many factors intervene and with a variety of possible outcomes depending on specific local conditions. A heuristic classification of calcium release event types has historically been established based on visual inspection of the event's spatio-temporal scale and the ability of the event to depolarize neighboring cells. These are: transients, waves, mini-waves, and sparks.

Cell **transients** are the normal cell function in which the intracellular calcium rises and triggers cell contraction. The release of calcium from the sarcoplasmic reticulum is homogeneous and synchronous. In a fraction of a second the intracellular calcium of the whole cell rises to maximum value and then decays to prepare for the next beat. Calcium **waves** are slow-propagating events in the sense that they are slower than a transient which is near instantaneous and does not propagate. The wave's slow-travelling speed allows for a neighboring cell to complete its refractory period. This implies that it can be stimulated twice by the wave which can produce a variety of undesired propagation faults that on the tissue scale result in cardiac malfunction. When a wave is propagating across a fraction of the cell and it is not capable of depolarizing neighboring cells it is referred to as a **mini-wave**. Calcium **sparks** (Fig. 4) are the smallest and the only type of event that can only be spontaneous whereas all other events can be both spontaneous and induced by other types of events. It is believed that sparks are a healthy regulation mechanism that allows for a flexible heart function. A lack of sparks implies a stiff dynamics and would induce heart pathologies [11]. On the other hand, waves are seen as unhealthy events because they are capable of altering the normal depolarizing front propagation patterns at the tissue level [12].

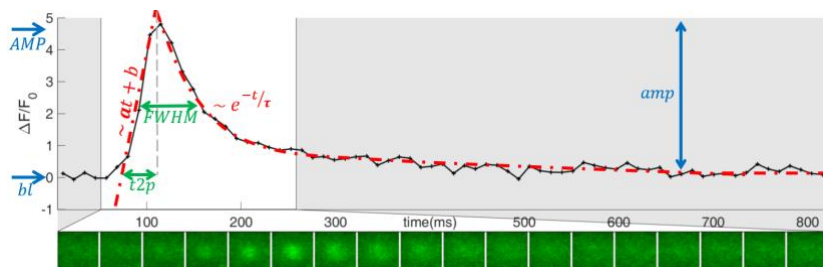


Fig. 4. Spark trace with image sequence and its morphological features. The spark trace was obtained by averaging the traces of many detected sparks and the regions of interest around the sparks were combined into a single image sequence revealing the calcium diffusion pattern. Morphological properties are absolute amplitude (AMP), relative amplitude (amp), baseline (bl), time to peak (t_{2p}), full width at half maximum (FWHM), rate of rise (a , in linear model), decay time (τ , in exponential model). Spatial resolution is of $0.23 \mu\text{m}/\text{pix}$ and temporal resolution of $11.63 \text{ ms}/\text{frame}$.

We developed a method to segment events in line scans and classify them by means of their morphological features (Fig. 5). The method made use of a space-time dependent baseline fluorescence computation based on a sliding window and a wavelet-based event detection, which allowed detecting events with a wide range of sizes and temporal scales. A set of features was measured for each detected event, and a decision tree was trained using these features to classify the detected intensity events into one of 5 categories: stimulated

or spontaneous transients, waves, mini-waves, sparks, and a sixth category reserved for discarded detection false positives. This line scan event detector and classifier led to the important finding that promotion of calcium intake by the SERCA pump into the sarcoplasmic reticulum breaks down calcium waves into separate smaller waves which suppresses ventricular tachycardia [13].

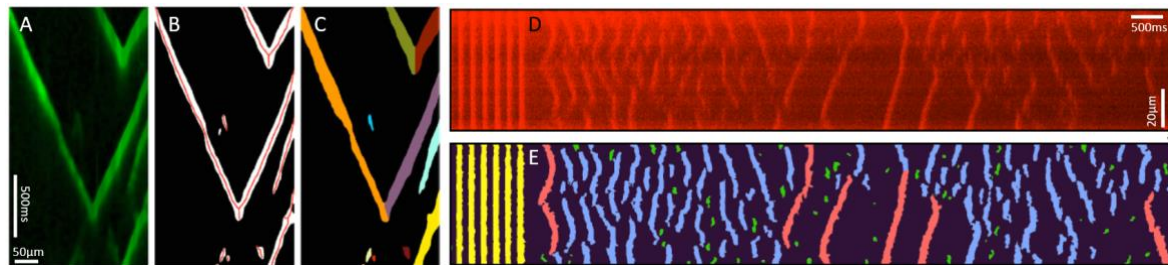


Fig. 5. Event detection and classification in line scans. A) Region of interest in calcium fluorescence in line scan. B) detection and skeletonization of events. C) Segmentation according to linear fits. D) Reference complete line scan. E) Detected and classified events: stimulated transients (yellow), waves (red), mini-waves (blue) and sparks (green).

The wavelet-based event detection method that we developed was then extended to frame scan temporal sequences and was specialized into a spark detection algorithm. The algorithm relies on a very sensitive detection step (ensuring no false negatives but allowing false positives), combined with a posterior filtering step (to remove false positives) based on user inputted set of parameters applied to the spark features. The features are an established set of morphological properties (see Fig. 4); absolute and relative amplitudes, the local baseline before the event, the time to peak intensity, the rate of rise, the rate of decay, the exponential decay constant, the full duration at half maximum and the full width at half maximum intensity. With this tool available, combined with the RyR2 detector, we were capable to colocalize sparks and RyR2 (Fig. 6). Our techniques have extensively been used in several studies linking low calcium levels in the sarcoplasmic reticulum and low membrane current to ageing [14,15]. A recent study has used it to relate the spark location to the number of RyR2 clusters involved in the release unit [16]. The method has further been modified, used to characterize calcium transients and to link RyR2 cluster function to the appearance of alternans at the cellular level (see following section) and to establish that suppression of RyR2 function promotes cardiac alternans at the heart level [9,17].

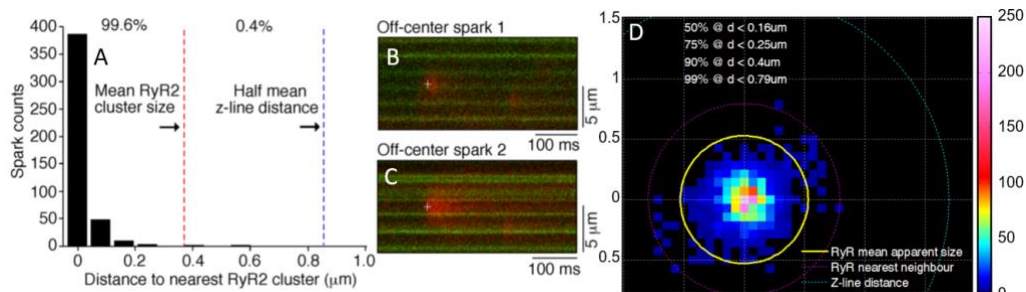


Fig. 6. RyR2 and spark colocalization. A) Histogram of detected sparks as a function of distance to nearest RyR2 cluster in line scans. B-C) Examples of rare off-center sparks in line scans (green RyR cluster, red calcium spark). D) 2D histogram of coordinates of detected sparks relative to closest detected RyR2 cluster center in frame scans.

In order to characterize propagating events in frame sequences, a calcium wave tracking pipeline was also developed. This involved using a frame-wise intensity-based segmentation of events, followed by a probabilistic approach to assign each object in one frame to objects in the next frame (Fig. 7). This method was further expanded and adapted to track any sort of fast moving objects (relative to the frame rate) and led to a quantification of mitochondria tracking [18,19].

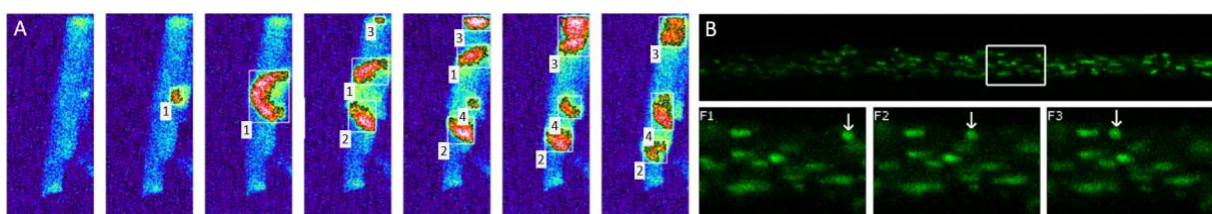


Fig. 7. Tracking algorithm. A) A sequence of frames shows calcium waves being created and their propagation. The algorithm successfully detects them, labels them and follows them throughout the sequence. B) Mitochondria travelling along a neuron axon. The three insets show three temporal frames where a single mitochondrion is being tracked.

2.c. Cellular Scale

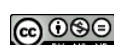
Normal function of a cardiomyocyte is to respond to a neighboring cell action potential with a calcium transient. This transient triggers its own contraction and in turn the next neighboring cell to start the same process. A typical stress experiment for a single cell (or a group of cells) is to submit it (or them) to electrical stimuli at constant frequency and observe their response at different pacing frequencies.

With the aim of developing a quantification system for cell dynamics of human myocytes in response to drugs, Dr Hove-Madsen's research group established a total of six classes into which the dynamics of a cell can be classified according to its response to external stimuli. These six dynamical regimes are 1) **Regular**; the cell responds with a normal transient after each stimulus. 2) **Alternans**; the cell responds with a lower intensity transient every other stimulus. 3) **Phase-lock**; severe case of alternans in which every other stimulus there is no cell response. 4) **Wave**; the cell initiates a slow propagating event that lasts over several stimuli. 5) **Irregular**; the cell responds in an irregular fashion that does not correlate to the stimulus. 6) **Inactive**; the cell does not respond to the stimulus. This classification was aimed at then relating it to both intracellular event statistics and tissue scale dynamics.

In order to have an automated and robust classifier of cell dynamics, we turned to machine learning, where there exists a whole battery of classifiers available in the literature. The starting point was a training set of pre-classified 569 temporal fluorescence signals of cells under a particular stimulation frequency. The pre-classification was manually performed by three human experts who inspected the individual temporal signals one-by-one and assigned one of the 6 dynamical regime labels. Using the known stimulation frequency as a reference, we established a total of 9 features to describe these signals. These features were chosen quantities that were aimed at targeting each of the dynamical regimes. They are statistical descriptors such as the coefficient of variation of the time between detected peaks in the signal, the mean time between detected peaks in the signal over the pacing period, the intensity of the highest peak in the continuous wavelet transform, the total amplitude of the signal, the mean of the signal, the standard deviation of the signal, and the standard deviation of the baseline of the signal. We tested the whole range of machine learning classifiers available in the literature and compared them using cross validation of the training set. This method consists in dividing the training into random subsets, a fraction of which are used to train the classifier and then the classifier is tested with the remaining subsets. The process is repeated many times until all possible combinations are exhausted to finally produce an accuracy value of the classifier as the total ratio correctly classified in the different testing subsets. Over 30 different classifiers were tested, including variations in the different parameter settings within the classifier families; support vector machine family, k-nearest neighbors, simple decision trees, and ensemble methods. The final classifier chosen based on overall best performance was an unpruned random forest [20].

Our classifier led to important findings in the study of arrhythmia, including that low density lipoprotein concentration reduces sarcoplasmic reticulum load and reduces calcium transient amplitude and its regularity where as high density lipoprotein does not [21]. Other studies using this approach identified a mutation responsible of increased spontaneous calcium release and ultimately of increased risk of atrial fibrillation [15] and that adenosine receptor (A_{2A}) activation promotes alternans at the cellular level [22]. Moreover, in a different study, single cell dynamics and transient kinetics were successfully linked to myocardial infarction and premature ageing [23].

Alternans in cardiac myocytes has proved to be linked to cardiac pathologies such as ventricular fibrillation and sudden death but the hidden mechanisms that trigger this behavior and its consequences are yet fully understood. Two sub-classes of Alternans have been established by the literature [24], **Spatially Discordant Alternans**; the cell has two distinct spatial regions which activate separately and contribute to an alternant behavior, i.e. half the cell is contracting when the other half is at rest and vice-versa. **Spatially Concordant Alternans**; the alternans is not due to spatial differences, rather the whole cell has an alternating pulsation, i.e. one large transient followed by one smaller transient. As a continuation of the dynamical regime classifier, we showed that principal component analysis (PCA) is an exceptional tool for distinguishing between these types of alternans [25] (Fig. 8), on top of being capable of detecting other dynamical behaviors. Our work on characterizing alternans and quantifying it in line scan traces was extensively used by Dr. S.R.W. Chen's group which established the relationship between defects in the RyR2 at the molecular level and the emergence of alternans at the cellular level [26–28].



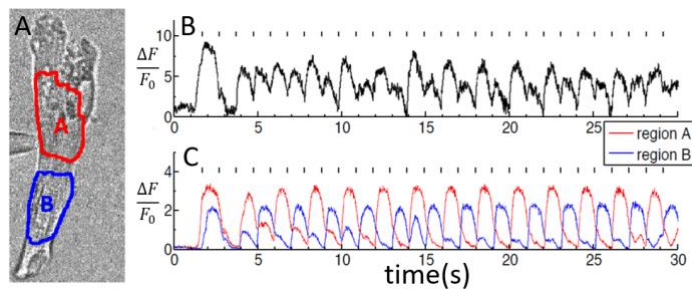


Fig. 8. Spatially discordant alternans is quantified by principal component analysis. A) Transmission image of a myocyte. B) Average fluorescence intensity of the image sequence. PCA resolves two regions in the image which are used to extract separate signals (C).

2.d. Culture Scale

Cardiac tissue is a complex network of connected myocytes that allows the propagation of the action potential that triggers the contraction of each individual cell. The study of patterns of the electrical propagation of this action potential in cardiac tissue is important for understand how pathologies at cellular level can affect myocardium function. Studies can be carried out using ex-vivo intact heart (removing a whole heart and keeping it alive while performing calcium imaging) or, for simplicity of equipment, tissue can be emulated by means of a cell culture (growing cells on a flat surface). Cultures also allow researchers to manipulate the surrounding media for instance by loading drugs to the culture or by adding mutated cells to regions of the culture. Just like for individual cells, cultures of cells are also electrically stimulated to test the system response and correct function. To do this, pair of electrodes are placed at one side of the culture and an electrical pulse triggers an action potential. Experimentalists can obtain image sequences where the brightness is proportional to calcium concentration and after each electrical pulse, a propagating calcium front is observed in the culture.

The individual images in the image sequences resulting from the calcium fronts in cardiac myocyte cultures are extremely noisy. Observing the presence of individual cells requires for the whole sequence to be viewed at a high frame rate (Fig. 9A). The usual approach when a single image does not contain enough information to reveal sharp edges is to take the mean of several images. In our case, to tackle the segmentation problem, we exploited the fact that cells are sitting on a flat surface and tend to be thicker around the center where the nucleus is, combined with the fact that the focal-plane is slightly above the culture dish, each cell has a larger portion within the focal-plane around the center than around the edges and therefore we register more light from the center than from the edges. As these are excitable cells, which throughout the sequence have an oscillatory behavior, a much better approach is to use the variance of the calcium concentration as an indicator of the positions where a cell is (at least a living cell). We defined the variability image as the standard deviation of the temporal signal in each pixel (Fig. 9B), which we then applied to a custom-built watershed-based method with an expected size constraint rule. We successfully used this technique to segment individual cells in the thousands counts (Fig. 9B), being able to then extract the temporal signal of each cell and use the dynamical regime classifier described in the previous section on each cell [25,29,30].

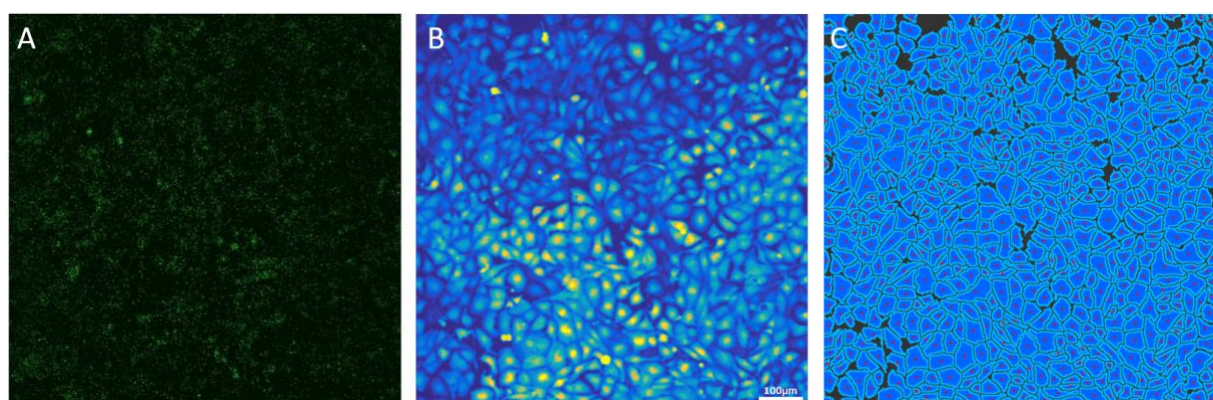


Fig. 9. A) Single frame of an image sequence of a culture of myocytes under external electrical periodic stimulation. B) Temporal variance of each pixel through time. C) Result of the segmentation algorithm resolves individual cells.

We further developed the technique to obtain the arrival time of each electrical stimulus at each pixel of the image based on the segmented cells and the dynamical regime classifiers described in the previous sections. This allowed us to characterize propagation dynamics and at the same time to classify the propagation amongst a set of predefined cases. These cases were set with the aim of establishing a connection between the individual cellular calcium dynamics and the properties of the propagating fronts (see Fig. 10). The four cases are 1) **Regular**; a flat front that is originated at the field electrodes, 2) **Reentry**; a flat front that is originated elsewhere, 3) **Spiral**; a front with constant angular velocity different to zero, 4) **Combined**; either non-constant angular velocity or a combination of various fronts. The spiral front dynamics are the cause of pathologies such as cardiac fibrillation. The origin of this spiral dynamics is a region in the network that is blocking the transmission of a front which causes the front to bend around the area. A spiral front can then cause a permanent activity around the area and the breaking of future fronts arriving at the region.

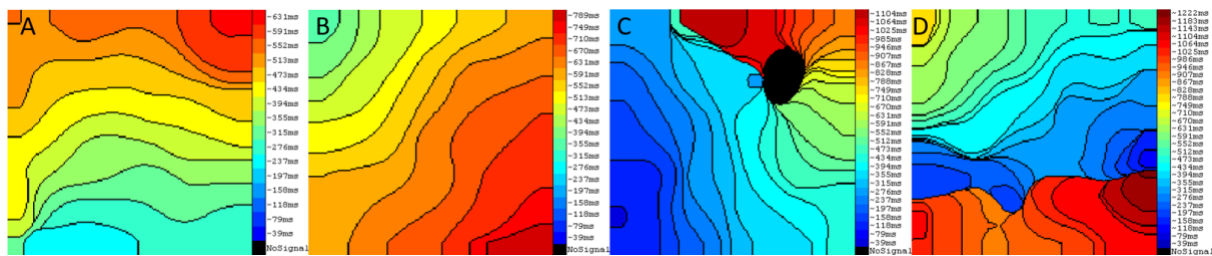


Fig. 10. Examples of different front propagation in a culture. A) Planar front. B) Reentry front. C) Spiral front. D) Irregular front.

3. Conclusion

The work summarized here and previously published in the thesis [4] belongs to the biomedical engineering discipline, focusing on the engineering perspective of applying physics and mathematics to solve biological and medical problems. Specifically, we frame our contributions in the field of computational translational cardiology, attempting to connect molecular mechanisms in cardiac cells to cardiac disease, by developing signal and image-processing methods as well as machine-learning methods that are scalable through the different scales. This computational approach allows for a quantitative, robust, and reproducible analysis of experimental data and allows us to obtain results that otherwise would not be possible by means of traditional manual methods.

The results of this work provide specific insight into different cell mechanisms that have an important impact at the clinical level. In particular, we gain a deeper knowledge of cell processes related to cardiac arrhythmia, fibrillation phenomena, the emergence of alternans and anomalies in calcium handling due to cell ageing. The specific contributions of the summarized studies were providing the image processing tools that allowed for the quantitative and reproducible analysis of images and image sequences obtained from scanning confocal fluorescence microscopy, stimulated emission depletion microscopy, total internal reflection fluorescence microscopy and epifluorescence microscopes.

Acknowledgements

The authors would like to thank the collaborators that provided experimental image sets that allowed for this work. They are Dr. Leif Hove-Madsen from the Biomedical Research Institute Barcelona Centre IIBB-CSIC in Barcelona, Prof. S. R. Wayne Chen from the Department of Physiology and Pharmacology in the Libin Cardiovascular Institute of Alberta, University of Calgary, Dr. Peter P. Jones from the Department of Physiology in the University of Otago, New Zealand, and Prof. Glen Tibbits from the Department of Biomedical Physiology & Kinesiology at the Simon Fraser University in Vancouver. Financial support was provided by the Government of Spain under projects DPI2009-06999 and DPI2013-44584-R.

